

## Techno-Economic Sensitivity Analysis of Integrated CCS–EOR for a 1,000 MW Ultra-Supercritical Coal-Fired Power Plant in Indonesia

Raden Ricko Satriyo\*, Renanto, Rendra Panca Anugraha, Roudlotus Salwa Aulia, Galuh Ferlianes Lestari

*Department of Chemical Engineering Institut Teknologi Sepuluh Nopember, Surabaya, East Java, 60111, Indonesia*

### Article history:

Submitted 27 February 2026  
Revision 27 March 2026  
Accepted 29 March 2026  
Online 1 April 2026

**ABSTRACT:** Coal-fired power plants supply 60% of Indonesia's electricity and are major CO<sub>2</sub> sources. Integrating Carbon Capture and Storage with Enhanced Oil Recovery (CCS-EOR) offers a decarbonization pathway with economic benefits. This study evaluates techno-economic performance of an integrated CCS-EOR system for a 1,000 MW ultra-supercritical coal plant in Indonesia, simulated using Aspen HYSYS V14 automated with Python. A solvent blend of 35 wt% MDEA and 15 wt% PZ was used. Four parameters, minimum approach temperature (10–20°C), CO<sub>2</sub> removal efficiency (85–95%), absorber inlet gas velocity (2–2.5 m/s), and stripper Murphree efficiency (0.4–0.8) were varied across full factorial combinations, generating 162 scenarios. Four optimal scenarios were identified via multi-method optimization and assessed for economic feasibility at pipeline distances of 50–200 km. In the base case (90% removal), the system captured 5.66 million tons CO<sub>2</sub>/year, with 28.91% energy penalty, Levelized Cost of CO<sub>2</sub> (LCoC) of -\$64.53/ton, and Net Present Value (NPV) of \$2.07 billion. CO<sub>2</sub> removal efficiency most influences LCoC, while  $\Delta T_{min}$  most affects energy penalty. The Balanced Optimal scenario (LCoC -\$65.65/ton, energy penalty 28.75%, NPV \$2.20 billion) is recommended and remains viable up to 200 km.

**Keywords:** Aspen HYSYS; Carbon Capture and Storage (CCS); MDEA; Python automation; techno-economic analysis

### 1. Introduction

Climate change resulting from greenhouse gas emissions, particularly carbon dioxide (CO<sub>2</sub>), poses the greatest environmental challenge facing the world today. Indonesia is one of the countries with the highest emission levels in Southeast Asia and has committed to achieving Net Zero Emission (NZE) by 2060 through its Enhanced Nationally Determined Contribution (NDC) under the UNFCCC, with an emission reduction target of 31.89–43.2% by 2030 (Government of Indonesia, 2022). However, the national energy sector's dependence on coal remains very high, reaching 40.46% of the primary energy mix in 2023, with coal-fired power plants (CFPPs) accounting for approximately 60% of national electricity production (IESR, 2024). With each 1,000 MW CFPP unit is estimated to generate around 6 million tons of CO<sub>2</sub> per year. This situation underscores the urgency of reducing emissions in the electricity sector. Carbon Capture and Storage (CCS) technology is considered one of the strategies capable of reducing 85–95% of CO<sub>2</sub> emissions from stationary sources without necessitating the premature shutdown of power plant operations (IEA, 2021; Mahidin et al., 2025).

Post-combustion technology based on chemical absorption using amine solvents has the highest

Technology Readiness Level (TRL), which is 9, and has been proven applicable to existing coal-fired power plants with relatively minimal modifications (Bui et al., 2018). Studies consistently demonstrate that the MDEA-PZ blend results in 20–25% lower regeneration energy consumption compared to MEA, with a higher CO<sub>2</sub> loading capacity (Rochelle et al., 2011; Rubin et al., 2015). Research on amine solvent configurations for CO<sub>2</sub> absorption, including DEA and MDEA-based systems, continues to advance process understanding in the Indonesian context (Pamungkas et al., 2025; Sussatrio et al., 2024). The characteristics of Indonesian coal, including calorific value and flue gas composition, are well documented and provide reliable simulation inputs (Febriani et al., 2024). In the context of storage, depleted oil and gas reservoirs are considered the most economical option due to the existing infrastructure that can be utilized and the potential for additional revenue from Enhanced Oil Recovery (EOR) schemes (Wei et al., 2023; Jarrell et al., 2002). Research on alternative separation technologies such as polymeric membranes continues to advance, although it has not yet reached a level of commercial maturity equivalent to absorption technology (Nyamiati et al., 2023). Adisasmito et al. (2023) conducted a techno-economic evaluation of CCS retrofitting on six coal-fired power plants in

\* Corresponding Author

Email address: [raden.satriyo@its.ac.id](mailto:raden.satriyo@its.ac.id)

Indonesia; however, this research was limited to calculating the Levelized Cost of Electricity without parametric optimization or multi-scenario analysis.

Based on this research gap, this study aims to develop a comprehensive techno-economic evaluation methodology for an integrated CCS system on a 1,000 MW ultra-supercritical coal-fired power plant in Indonesia. The novelty of this research lies in the integration of Aspen HYSYS V14 simulation automation with Python via the COM interface to efficiently evaluate 162 combinations of operating scenarios, encompassing variations in the minimum approach temperature of the lean/rich heat exchanger, CO<sub>2</sub> removal efficiency, Murphree stripper efficiency, and absorber inlet gas velocity. A multi-method optimization approach, comprising Pareto frontier analysis, single-objective optimization, lexicographic optimization, and constraint-based selection, was applied to identify four representative scenarios relevant to various stakeholders. These scenarios were then further evaluated for the influence of feasibility at each distance. The specific objectives of this research are to develop an integrated CCS-EOR process simulation model using Aspen HYSYS, automate parameter variations and cost calculations via Python, analyze the sensitivity of process parameters to energy penalty and Levelized Cost of CO<sub>2</sub> (LCoC), and provide technical and economic recommendations for CCS implementation on coal-fired power plants in Indonesia, including the identification of the critical pipeline distance beyond which project feasibility is no longer viable.

extraction from the medium-pressure turbine stage (3–5 bar) for reboiler heat duty, converted to electrical equivalent using a thermal efficiency of 0.333 and the facility's actual electrical consumption, divided by the total plant power output (Irfan, 2021). EOR surface facilities and well conversion are included in the storage capital expenditure (CAPEX). Meanwhile, operating expenses (OPEX) include maintenance and abandonment and site restoration (ASR) costs (Yasmin, 2021). Figure 1 includes explicit system boundary.

The flue gas data used as the simulation feed were obtained from Adisasmito et al. (2023), a study conducted with direct collaboration of PT PLN (Persero). The paper uses data collected from six actual Indonesian coal-fired power plants currently in operation. Consequently, the flue gas parameters for the 1,000 MW ultra-supercritical unit as seen in Table 1 are actual measured operating conditions of a PLN-operated power plant, not simulated values. This confirms that the simulation feed conditions are representative of real Indonesian CFPP operation under seawater FGD pretreatment.

The CO<sub>2</sub> concentration of 13 mol% is consistent with the typical range for coal combustion, particularly considering that Indonesian coal is predominantly low-rank, which produces CO<sub>2</sub> as a major combustion product (Adisasmito et al., 2023; Bui et al., 2018; Febriani et al., 2024). Particulate matter and bulk NO<sub>x</sub> are assumed removed by upstream FGD units, consistent with standard PLN power plant operational practice.

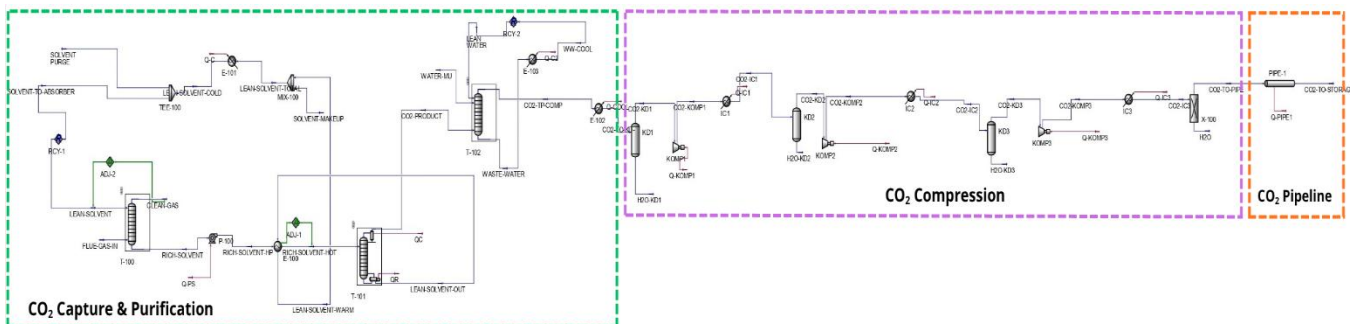


Figure 1. Flowsheet for Carbon Capture and Storage (CCS) Boundary System

## 2. Materials and Methods

### 2.1. System Configuration and Flue Gas Data

This study examines an integrated end-to-end carbon capture and storage (CCS) system consisting of four units: post-combustion chemical absorption-based CO<sub>2</sub> capture, multi-stage CO<sub>2</sub> purification and compression, pipeline transportation, and CO<sub>2</sub>-EOR storage in a depleted oil reservoir. The system boundary of this study begins downstream of the seawater flue gas desulfurization (FGD) unit; FGD capital and operating costs are therefore excluded from the analysis. The energy penalty is derived from the parasitic power demand, which is the sum of the equivalent electrical power loss resulting from steam

The residual SO<sub>2</sub> of 0.10 mol% is explicitly modeled; heat-stable salt formation is mitigated by maintaining absorber outlet temperatures below 60°C. The wash water column reduces acid gases to below 100 ppmv, meeting EOR injection requirements (NETL, 2019).

**Table 1.** Flue Gas Data (Adisasmito et al., 2023)

Parameter	Value	Parameter	Value
Temperature (°C)	64	CO <sub>2</sub> (mole fraction)	13%
Flow rate (Nm <sup>3</sup> /hour)	3,279,214	N <sub>2</sub> (mole fraction)	70.4%
Pressure (bar)	1.03	H <sub>2</sub> O (mole fraction)	11.9%
		O <sub>2</sub> (mole fraction)	4.59%
		SO <sub>2</sub> (mole fraction)	0.1%

## 2.2. Process Modeling and Simulation

The entire system was modeled using Aspen HYSYS V14 with a rate-based approach for the absorber and stripper units. Two thermodynamic fluid packages were employed based on the chemical characteristics of each process section. The Acid Gas – Chemical Solvents package was used for units involving amine–CO<sub>2</sub>–H<sub>2</sub>O chemical reactions specifically the absorber, stripper, and solvent heat exchangers. The Peng-Robinson equation of state was used for the compression unit and pipeline section, which operate under dense-phase conditions approaching supercritical pressure where its thermodynamic accuracy is critical for predicting compressor power consumption and pipeline pressure drop (Aspelund et al., 2006). The solvent used is a mixture of 35 wt% MDEA and 15 wt% PZ (piperazine), with PZ acting as a kinetic promoter that increases the CO<sub>2</sub> absorption rate 3–5 times through carbamate formation (Bishnoi & Rochelle, 2000; Rochelle, 2009).

### 2.2.1 Equipment Sizing

The absorber and stripper columns are designed as packed columns using Mellapak 250Y structured packing (specific interfacial area: 250 m<sup>2</sup>/m<sup>3</sup>), which offers low pressure drop and high gas-liquid contact efficiency (Pershen, 2025). The absorber is configured with a total packing height of 50 m, equivalent to 20 theoretical stages at a Murphree efficiency of 0.8; the stripper uses the same packing type over 25 m (15 theoretical stages). Column diameter was calculated from the volumetric gas flow rate and target superficial gas velocity using Eq 1 and 2 from Pershen (2025).

$$A = \frac{\dot{V}_{gas}}{v_{gas}} \quad (1)$$

$$D = \sqrt{\frac{4 \cdot A}{\pi}} \quad (2)$$

where A is the column cross-sectional area (m<sup>2</sup>),  $\dot{V}_{gas}$  is the volumetric gas flow rate from the HYSYS simulation (m<sup>3</sup>/h),  $v_{gas}$  is the target superficial gas velocity (m/s), and D is the column diameter (m). For the absorber, gas velocity is an independent variable varied between 2.0 and 2.5 m/s. For the stripper, a superficial vapor velocity of approximately 1.5 m/s is used. The absorber operates at a flooding fraction of 70% at the base case inlet gas velocity of 2.5 m/s, consistent with the recommended design range of 60–80% for structured packing (NETL, 2015).

The packing cost and column shell cost are treated as separate components in the power-law scaling because they scale differently: packing cost scales with column diameter ( $M = 1.70$ ) while the shell cost scales with the total tangent-to-tangent (TT) height ( $M = 0.60$ ; Smith, 2016; Turton et al., 2012). The TT height of the stripper depends on the required packing height, which is in turn governed by the Murphree stage efficiency, an independent

variable in this study (0.4, 0.6, 0.8). From the equipment sizing aspect, the absorber requires a diameter of 23.5 m for a single-unit configuration, which is practically infeasible considering that commercial-scale CCS absorbers such as those at Boundary Dam and Petra Nova operate with diameters of 10–15 m (NETL, 2015; Boot-Handford et al., 2014). A parallel solution with two absorber units, each with a diameter of 16.62 m, is deemed constructively feasible. The stripper has a diameter of 7.65 m and a height of 25 m, which falls within standard industry ranges.

Heat transfer area for all shell-and-tube heat exchangers including the lean/rich HEX, lean cooler, intercoolers, reboiler, and condenser was calculated using the following equation from Pershen (2025):

$$A = \frac{Q}{U \cdot \Delta T_{LMTD}} \quad (3)$$

where A is the heat transfer area (m<sup>2</sup>), Q is the heat duty from the HYSYS simulation (kW), U is the overall heat transfer coefficient (kW/m<sup>2</sup>K; typically 0.50–0.73 kW/m<sup>2</sup>K for shell-and-tube HEX; Pershen, 2025), and  $\Delta T_{LMTD}$  is the log mean temperature difference (K). The lean/rich HEX uses  $\Delta T_{min} = 10^\circ\text{C}$  as the base case operating constraint, which achieves 70–75% internal heat recovery of the sensible heat requirement. All resulting heat transfer areas (m<sup>2</sup>) are used directly as the capacity measure Q in the power-law scaling equation. The key parameters and assumptions for the base case configuration are summarized in Table 2.

**Table 2.** Base Case Configuration Specifications

Unit	Parameter	Value	Reference
CO <sub>2</sub> Capture	<i>Packing</i>	Mellapak	Park & Øi
	absorber	250Y	(2017)
	Inlet gas velocity (m/s)	2.5	NETL (2015)
	Stripper pressure (bar)	2	Adisasmito (2023)
	<i>Reboiler</i> temperature (°C)	120	Rochelle (2009)
	$\Delta T$ min. HX (°C)	10	Rubin et al. (2015)
Compression	<i>Murphree efficiency</i>	0.8	
	Number of stages	3	
	<i>Pressure outlet (bar)</i>	145	
Pipeline	<i>Isentropic efficiency (%)</i>	75–80	
	Nominal diameter (mm)	450	Peletiri et al. (2018)
	Material	Carbon steel X45/X80	ASME B31.4
Storage-EOR	Incremental recovery	2 bbl/ton CO <sub>2</sub>	Jarrell et al. (2002)

Compressor shaft power was extracted directly from the HYSYS simulation output using isentropic compression equations with 75–80% isentropic efficiency across three stages with intercooling to 30–50°C between stages. The pressure ratio distribution is 5:5:3, designed based on the principle of equal work distribution to prevent the formation of a two-phase region at the critical compression point in the final stage (Li et al., 2019). , from 2 bar stripper outlet to 145 bar dense-phase transportation pressure. (NETL, 2015). The simulation-derived power value (kJ/h) is used directly as the capacity measure Q in the power-law scaling. Pipeline pressure drop was modeled using the Beggs and Brill equation as implemented in HYSYS, yielding a specific pressure drop of 0.73 bar/km at the 50 km base case within the acceptable range of 0.5–1.0 bar/km for 450 mm diameter CO<sub>2</sub> pipeline in dense phase at 145 bar (Peletiri et al., 2017, 2018).

### 2.3. Cost Estimation

The CAPEX for the capture and compression units was obtained from the Aspen Process Economic Analyzer (APEA V14, Q1 2022 pricing basis) based on the physical parameters resulting from sizing in Aspen HYSYS. Meanwhile, the CAPEX for the pipeline was calculated using the methodology of Handogo et al. (2022), and the CAPEX for storage refers to NETL (2015). OPEX includes variable costs (steam, electricity, cooling water, and solvent make-up) and fixed costs (maintenance at 4% of CAPEX per year). Cost estimation across different operating scenarios was performed using the power law scaling method (Eq 4) (Smith, 2016).

$$C_E = C_B \left( \frac{Q}{Q_B} \right)^M \quad (4)$$

where C<sub>E</sub> is equipment cost with capacity Q, C<sub>B</sub> is the base case equipment cost from the APEA V14 reference model (Q1 2022 basis), Q<sub>B</sub> is the base case capacity parameter, Q is this study's capacity parameter from HYSYS simulation, and M is the equipment-specific cost scaling exponent listed in Table 3. Also, the main economic assumptions used in the calculations for the carbon capture and storage system are presented in Table 3.

The steam cost of \$9.45/ton (Turton, 2012) represents the cost of low-pressure steam (3–5 bar, 143–151°C) extracted from the medium-pressure turbine stage of the host power plant. The energy penalty calculation separately and fully accounts for the opportunity cost of this steam extraction, calculated as the foregone electricity generation that would otherwise have been produced in the low-pressure turbine stage, using a thermal-to-electrical conversion efficiency of 0.30 for medium-pressure extraction (Rubin et al., 2015; Lucquiaud & Gibbins, 2011). The two cost items therefore represent distinct and complementary economic impacts: the steam cost captures the direct utility expenditure, while the energy penalty captures the lost revenue from reduced power output. Economic feasibility was evaluated using two indicators:

Levelized Cost of CO<sub>2</sub> (LCoC), and Net Present Value (NPV). The energy penalty was also calculated as the percentage reduction in the power plant's net output due to the CCS system (IPCC, 2005).

### 2.4. Simulation Automation and Research Variables

Aspen HYSYS V14 simulation automation was implemented in Python using the COM (Component Object Model) interface via the win32com.client library. Additional libraries are pandas and numpy (data management), scipy (numerical calculations), matplotlib (visualization), and openpyxl (Excel export). The automation workflow begins by opening the HYSYS case file and iterating through all 162 parameter combinations.

**Table 3.** Economic Parameter

Cost Scaling Exponents			
Equipment	Capacity Measure	M	Reference
Column Packing (absorber, stripper, wash column)	Column diameter (m)	1.7	Smith (2016)
Column Shell (absorber, stripper, wash column)	TT height (m)	0.6	Turton et al. (2012)
Shell and Tube Heat Exchanger (lean/rich heat exchanger, coolers, intercoolers, reboiler, condenser)	Heat transfer area (m <sup>2</sup> )	0.68	Smith (2016)
Compressor (each stage, including motor)	Power (kJ/h)	0.46	Smith (2016)
Centrifugal Pump (including motor)	Power (kJ/h)	0.55	Smith (2016)
KO Drum/Separator (vessel)	Height (m)	0.6	Turton et al. (2012)
Economic Parameter Assumptions			
Parameter	Value	Unit	Reference
Project lifetime / Construction/ Operation	25 / 5 / 20	Year	Abu-Zahra et al. (2007)
Discount rate	8.5	%	Sultan et al. (2021)
Operating hours per year	7,500	Hour	Abu-Zahra et al. (2007)
Steam cost	9.45	USD/ton	Turton (2012)
Electricity cost	0.061	USD/kWh	PLN (2025)
Carbon incentive	10	USD/ton CO <sub>2</sub>	IEF (2021)
Incremental EOR oil price	60	USD/bbl	ESDM (2025)

Each parameter is assigned via COM access to an Adjust block or spreadsheet cell. Structured wait times are

applied: 60 seconds after each Murphree efficiency change to allow full column recalculation, 5 seconds after gas velocity changes, and 0 seconds after  $\Delta T_{min}$  changes (as these are handled internally by HYSYS's Adjust block solver). Convergence is verified by polling the 'Simulation.Solver.CanSolve' and 'Simulation.Solver.IsSolving' flags at 5-second intervals with a 120-second timeout. If the solver is inactive and not solving, convergence is confirmed. If the timeout is exceeded, the scenario is logged as a warning and skipped via 'continue'. Output variables are then extracted from named HYSYS spreadsheet cells, with a fallback value of 0.0 in case of cell-read errors. Economic calculations are performed in Python, and results are exported to Excel. Each parameter-setting function returns a Boolean; a 'False' value triggers a skip without terminating the loop. All operations are recorded in a timestamped log file. The main loop's 'finally' block closes HYSYS unconditionally. No convergence failures were recorded across all 162 scenarios, with a total runtime of approximately 3 hours. A workflow diagram in general is provided in Figure 2.

Control variables were kept constant (solvent type, capture technology, transportation and storage type), while four independent variables were varied: heat exchanger minimum approach temperature (10°C, 12°C, 14°C, 16°C, 18°C, and 20°C), CO<sub>2</sub> recovery (85%, 90%, and 95%), absorber inlet gas velocity (2, 2.25, and 2.5 m/s), and stripper Murphree efficiency (0.4, 0.6, and 0.8). These four variables will be combined to generate 162 variations. From the 162 evaluated combinations, four representative scenarios were then selected using rule-based criteria: the lowest LCoC scenario (single-objective optimization), the highest efficiency scenario (lexicographic optimization), the balanced optimal scenario (knee point of the Pareto front), and the constraint-based scenario (conservative industry parameters). The parameter combinations of these four optimal scenarios were subsequently used as the basis for a robustness evaluation by varying pipeline transportation distance across four values: 50, 100, 150, and 200 km. The dependent variables evaluated include energy penalty, LCoC, and NPV.

### 2.5. Sensitivity Analysis and Model Validation

Sensitivity analysis was conducted using the One-at-a-Time (OAT) method by varying a single parameter within its range while keeping other parameters at base case conditions. This was applied to analyze the influence of each parameter on the energy penalty and LCoC, as well as the effect of pipeline distance on NPV. The results of all scenarios were subsequently analyzed using the Pareto frontier to identify the trade-off between minimizing the energy penalty, maximizing CO<sub>2</sub> recovery, and minimizing LCoC simultaneously. From the Pareto frontier, four main scenarios were selected based on rule-based criteria: lowest cost (minimum LCoC), highest efficiency (maximum recovery and minimum energy penalty), constraint (base

case conditions), and balanced optimal, selected through knee point identification.

Process model validation was performed by comparing the base case simulation results against reference data from NETL for regeneration energy consumption (GJ/ton CO<sub>2</sub>), solvent circulation rate, and absorber-stripper column temperature profiles. Economic model validation was conducted by comparing CAPEX, OPEX, and LCoC estimates against published CCS techno-economic studies from the IEA, DOE/NETL, and peer-reviewed academic literature of similar scale and configuration.

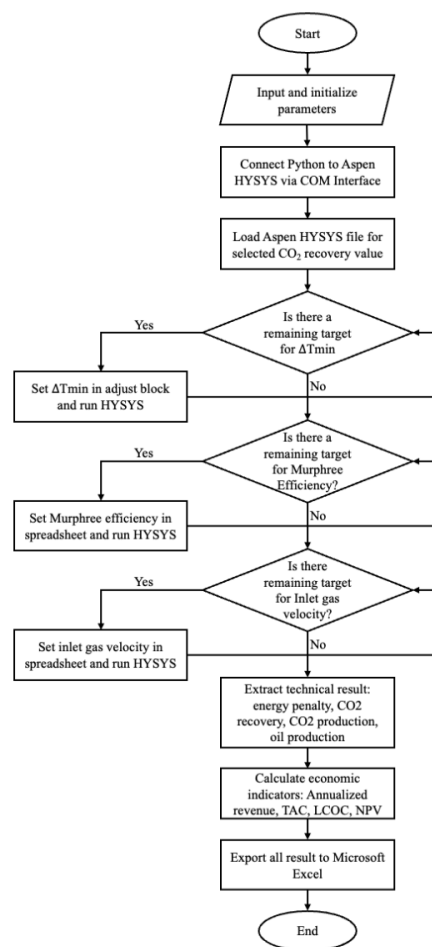


**Figure 2.** HYSYS-Python Automation Flowchart

## 3. Results and Discussion

### 3.1. Based Case System Performance and Model Validation

The base case simulation was conducted under standard operating conditions with a 90% CO<sub>2</sub> removal rate, a  $\Delta T_{min}$  of 10°C, a Murphree efficiency of 0.8, an inlet gas velocity of 2.5 m/s, and a pipeline distance of 50 km. The system utilized a solvent blend of 35 wt% MDEA and 15 wt% piperazine (PZ) as a kinetic absorption promoter. A

summary of the system's performance parameters under base case conditions is presented in Table 4.

**Table 4.** System Performance Parameters of the CCS-EOR System under Base Case Conditions

Techno-Economic Performance Parameters		
Parameter	Value	Unit
CO <sub>2</sub> Captured	5.66	Million tons/year
Energy Penalty	28.91	%
Specific Reboiler Duty	3.08	GJ/ton CO <sub>2</sub>
Total CAPEX	1,315.4	Million USD
Total Annual OPEX	241.9	Million USD/year
Annual Revenue	735.6	Million USD/year
LCoC	-64.53	USD/ton CO <sub>2</sub>
NPV	2,070.2	Million USD
Solvent Operating Parameters		
Parameter	Value	Unit
Solvent Circulation	7,919	Ton/hour
Solvent Degradation	0,00025	Kg solvent/ton CO <sub>2</sub> Captured
MDEA Make-Up	0.31	Ton/hour
PZ Make-Up	0.5	Ton/hour
Total Solvent Make-Up	0.81	Ton/hour
Water Make-Up	490	Ton/hour
Lean CO <sub>2</sub> loading	0.131	Mol CO <sub>2</sub> /mol solvent
Rich CO <sub>2</sub> loading	0.738	Mol CO <sub>2</sub> /mol solvent
L/G ratio	1.13	Kg/kg

### 3.1.1 Techno-Economic Performance Parameters

The system successfully captured 5.66 million tons of CO<sub>2</sub> per year from the total power plant emissions of 6.3 million tons of CO<sub>2</sub> per year, equivalent to a 90% capture rate. Total energy consumption reached 289.13 MW, resulting in an energy penalty of 28.91% relative to the power plant's net output. The system's specific energy consumption (SEC) of 3.08 GJ/ton CO<sub>2</sub> falls within the lower range of literature values for MDEA systems with a piperazine promoter, which is 3.0–4.0 GJ/ton CO<sub>2</sub> (Rochelle, 2009). The base case specific reboiler duty of 3.08 GJ/ton CO<sub>2</sub> represents a 20–25% improvement over conventional MEA systems (3.7–4.0 GJ/ton CO<sub>2</sub>; Rubin et al., 2015). The energy penalty of 28.91% is consistent with the range of 20–35% widely reported for post-combustion capture on coal-fired power plants (Rubin et al., 2015; NETL, 2015; IEA, 2021). Total project CAPEX of \$1,315.4 million is within the reference range of \$900–\$1,500 million for comparable 1,000 MW post-combustion CCS systems (NETL, 2015; Rubin et al., 2015), with total annual OPEX of \$241.9 million and annual revenue of \$735.6 million.

The resulting LCoC of -\$64.53/ton CO<sub>2</sub> and NPV of \$2,070.2 million confirm that the integrated CCS-EOR system is economically profitable under base case conditions. Model validation confirms that the CO<sub>2</sub> capture efficiency of 90% meets the ≥90% design criterion (Adisasmito et al., 2023; NETL, 2015; IEA, 2021). CO<sub>2</sub> product purity ≥99.99 vol% exceeds EOR injection specification of >95 vol% (NETL, 2019), with the higher

purity relative to Adisasmito et al. (2023) (97.47 wt%) attributable to the wash water column in this study.

### 3.1.2 Solvent Operating Conditions

The base case simulation produced the following key solvent operating parameters, which are reported here as simulation results and used for model validation. The solvent circulation rate was 7,919 ton/hour with an L/G ratio of 1.13 kg/kg, while the lean CO<sub>2</sub> loading was 0.131 mol CO<sub>2</sub>/mol amine and rich CO<sub>2</sub> loading was 0.738 mol CO<sub>2</sub>/mol amine, yielding a cyclic loading of 0.607 mol CO<sub>2</sub>/mol amine. MDEA and PZ make-up rates were 0.31 and 0.50 ton/hour, respectively, for a total solvent make-up of 0.81 ton/hour, with a water make-up of 490 ton/hour. The solvent degradation rate of 0.00025 kg solvent/ton CO<sub>2</sub> captured is well below the acceptable threshold of 0.5 kg/ton CO<sub>2</sub> for industrial amine capture plants (Rochelle, 2009), confirming that operating conditions (reboiler ≤120°C, absorber outlet ≤60°C) successfully minimize both thermal and oxidative degradation.

Model validation was performed by comparing simulation results with those from Adisasmito et al. (2023). The deviation in solvent circulation rate was 18.3% (7,919 vs. 9,693 ton/hour). The 18.3% lower solvent circulation rate in this study (7,919 vs. 9,693 ton/hour) is directly attributable to the higher CO<sub>2</sub> absorption capacity per unit of solvent for the 35%MDEA+15%PZ blend relative to the Shell-Cansolv formulation used by Adisasmito et al. (2023). The piperazine promoter increases the effective CO<sub>2</sub> loading per mole of amine (higher cyclic loading of 0.607 mol CO<sub>2</sub>/mol amine), enabling a lower circulation rate to achieve the same 90% capture target. This is consistent with the well-documented advantage of PZ-promoted MDEA systems over conventional MEA or proprietary amine blends in reducing solvent circulation requirements (Rochelle, 2009; Rochelle et al., 2011). Comparing this study with other CCS research adds to the model's credibility. Lean CO<sub>2</sub> loading of 0.131 and rich loading of 0.738 mol CO<sub>2</sub>/mol amine are consistent with the validated performance range for MDEA-PZ blends, where lean loading of 0.10–0.15 ensures adequate driving force for absorption, and rich loading of 0.60–0.80 reflects high absorption capacity per cycle (Rochelle, 2009; Bishnoi & Rochelle, 2000). L/G ratio of 1.13 kg/kg is within the optimal range of 1.0–1.5 kg/kg for MDEA-PZ systems, consistent with Rochelle (2009), who notes that lower L/G ratios are achievable with higher-loading PZ-promoted solvents relative to MEA (typical L/G 1.5–2.0 kg/kg).

### 3.2. Sensitivity Analysis of Process Parameters

Sensitivity analysis was conducted using the One-at-a-Time (OAT) method on four operating parameters: CO<sub>2</sub> removal percentage (85–95%), heat exchanger ΔT<sub>min</sub> (10–20°C), Murphree efficiency in the stripper (0.4–0.8), and absorber inlet gas velocity (2–2.5 m/s). The two performance indicators analyzed were LCoC and energy penalty. The sensitivity analysis results are consolidated into two combined figures. Figure 3 presents the effect of all four parameters, % CO<sub>2</sub> removal rate, heat exchanger

$\Delta T_{min}$ , absorber inlet gas velocity, and stripper Murphree efficiency on the Levelized Cost of CO<sub>2</sub> (LCoC). Figure 4

presents the combined effects of  $\Delta T_{min}$  and Murphree efficiency on the energy penalty.

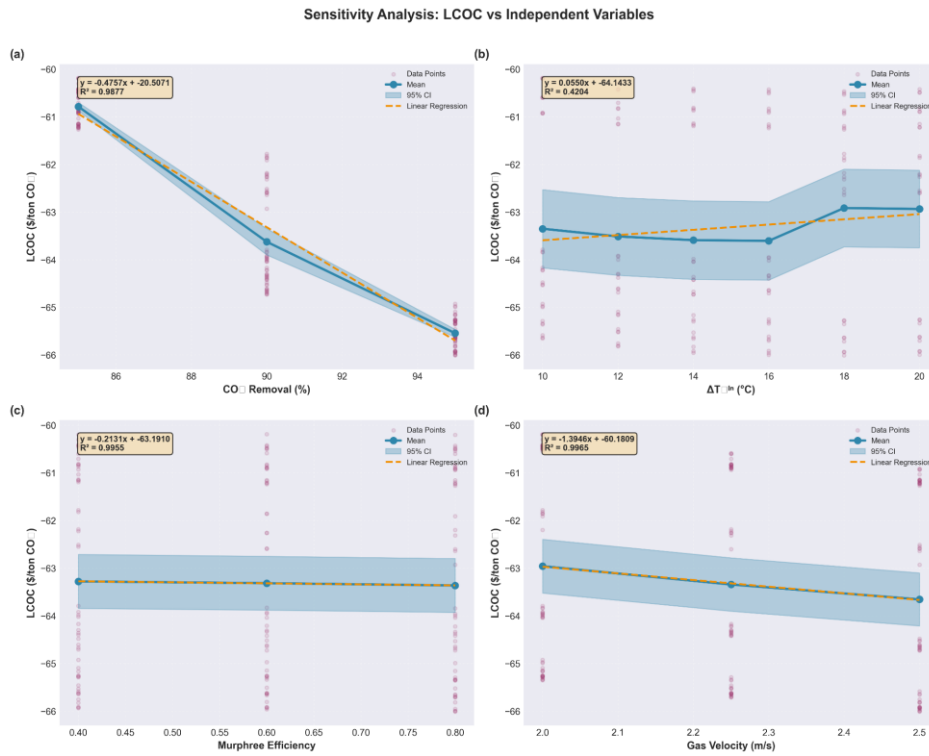


**Figure. 3** Effect of All Four Parameters on the Levelized Cost of CO<sub>2</sub> (LCoC): (a) Effect of % CO<sub>2</sub> removal; (b) Effect of %  $\Delta T_{min}$  HEX; (c) Effect of Murphree efficiency in Stripper; (d) Effect of Gas velocity in Absorber.

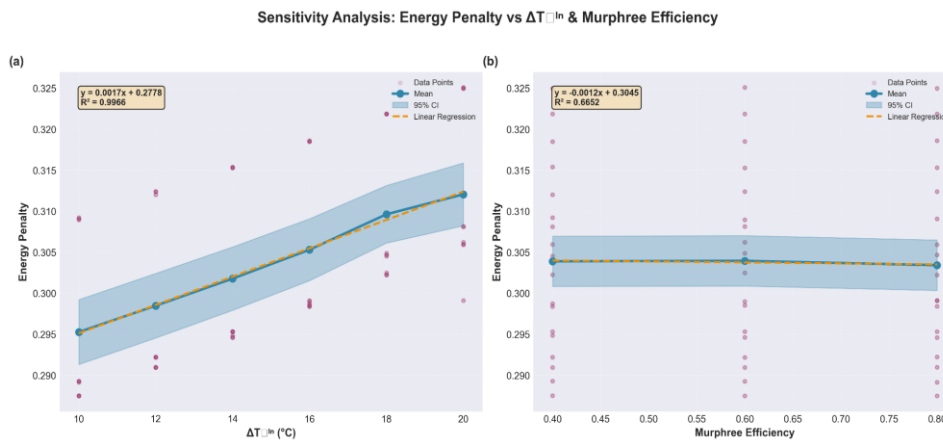


**Figure. 4** Effect of  $\Delta T_{min}$  and Murphree efficiency on the energy penalty: (a) Effect of  $\Delta T_{min}$  HEX; (b) Effect of Murphree efficiency in Stripper

A quantitative summary of all sensitivity gradients and regression equations is provided in Table 5.

### 3.2.1 Effect of % CO<sub>2</sub> Removal on LCoC and Energy Penalty

The % CO<sub>2</sub> removal parameter is the most sensitive parameter to LCoC, as shown in Figure 3. The linear regression equation obtained is as follows.

$$LCoC = -0.4757 \times \%Removal - 20.5071 \quad (R^2 = 0.9877) \quad (5)$$

where LCoC is the Levelized Cost of CO<sub>2</sub> (USD/ton CO<sub>2</sub>) and %Removal is the CO<sub>2</sub> removal efficiency (%). The LCoC value increased from  $-\$60.93/\text{ton}$  at 85% removal to  $-\$65.69/\text{ton}$  at 95% removal, an increase of 7.8%. This dominance of CO<sub>2</sub> removal rate on LCoC is consistent with Rubin et al. (2015), who identify capture efficiency as the most influential parameter due to its simultaneous effect on both revenue and cost.

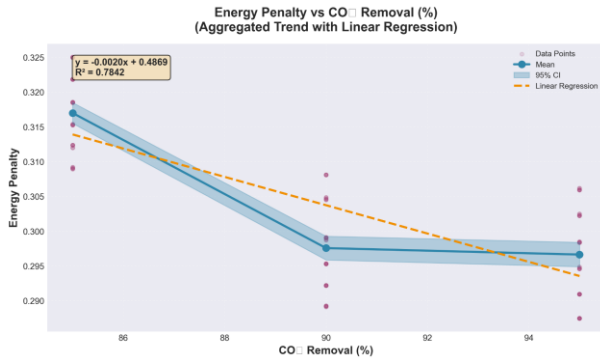


Figure 5. Effect of % CO<sub>2</sub> Removal on Energy Penalty

A counter-intuitive finding was obtained regarding the relationship between % CO<sub>2</sub> removal and energy penalty. Increasing the removal rate from 85% to 95% actually resulted in a decrease in the energy penalty from 31.68% to 29.65% (a decrease of 2.03 percentage points), as shown in Figure 5 with the following linear regression equation (Eq 6).

$$EP = -0.002 \times \% \text{Removal} + 0.4869 \quad (R^2 = 0.7842) \quad (6)$$

where EP is the energy penalty (dimensionless fraction).

Table 5. Summary of Operating Parameter Sensitivity on System Performance

Parameter	Effect on LCoC (\$/ton per unit)	Effect on Energy Penalty (% per unit)
% CO <sub>2</sub> removal	-0.48 per 1%	-0.20 per 1%
Gas velocity in Absorber	-1.39 per m/s	0
$\Delta T_{\min}$ HEX	+0.055 per °C	+0.17 per °C
Murphree efficiency in Stripper	-0.21 per unit	-0.12 per unit

This phenomenon occurs because, in the Aspen HYSYS simulation with fixed operational constraints (reboiler temperature of 120°C and overhead CO<sub>2</sub> purity of 97 wt%), the increase in the removal rate causes the system to operate under thermodynamically more optimal internal conditions. At high removal rates, the higher rich CO<sub>2</sub> loading results in lower specific energy per mole of CO<sub>2</sub> regenerated due to more optimal distribution and loading in the heat integration (Rochelle, 2009; Pershen, 2025). Similar non-monotonic behavior was reported by Rochelle (2009) for amine systems with kinetic promoters such as piperazine, indicating that specific energy consumption can change non-linearly depending on operating conditions and system constraints.

### 3.2.2 Effect of Heat Exchanger $\Delta T_{\min}$ on LCoC and Energy Penalty

The  $\Delta T_{\min}$  parameter has a very small impact on LCoC, as shown in Figure 3. The linear regression equation obtained is as follows (Eq 7).

$$LCoC = 0.055 \times \Delta T_{\min} - 64.1433 \quad (R^2 = 0.4204) \quad (7)$$

where  $\Delta T_{\min}$  is the minimum approach temperature in lean/rich heat exchanger (°C). A total change of only \$0.26/ton was obtained over the 10–20°C range. The reason is that although the heat exchanger CAPEX decreases with increasing  $\Delta T_{\min}$  (due to a smaller heat transfer area), this saving is offset by the increase in energy OPEX, resulting in a minimal net effect on LCoC. This finding is consistent with the study by Smith (2016) on the fundamental trade-off between capital cost and energy cost in heat exchanger network design.

Conversely, the  $\Delta T_{\min}$  parameter is the most sensitive parameter to the energy penalty, as shown in Figure 4 with the following linear regression equation (Eq 8).

$$EP = 0.0017 \times \Delta T_{\min} + 0.2778 \quad (R^2 = 0.9966) \quad (8)$$

Each 1°C increase in  $\Delta T_{\min}$  raises the energy penalty by 0.17 percentage points, equivalent to an increase in absolute energy consumption of approximately 1.7 MW. This is explained through the principle of pinch analysis, where a larger  $\Delta T_{\min}$  reduces the effectiveness of internal heat recovery in the lean-rich heat exchanger; at a  $\Delta T_{\min}$  of 10°C, heat recovery reaches 70–75% of the sensible heat requirement, whereas at a  $\Delta T_{\min}$  of 20°C it drops to 60–65% (Smith, 2016; Pershen, 2025). The unrecovered heat gap must be supplied by external steam, which directly increases the power plant derating.

### 3.2.3 Effect of Absorber Inlet Gas Velocity on LCoC and Energy Penalty

The absorber inlet gas velocity has a significant effect on LCoC through its impact on equipment sizing, as shown in Figure 3 with the following linear regression equation (Eq 9).

$$LCoC = -1.3946 \times v - 60.1809 \quad (R^2 = 0.9965) \quad (9)$$

Where  $v$  is the maximum allowable vapor velocity, based on the gross (total) column cross-sectional area (m/s). This indicates that every 1 m/s increase in gas velocity results in a decrease in LCoC of \$1.39/ton CO<sub>2</sub>. This is consistent with Park & Øi (2017), who demonstrate significant absorber CAPEX reduction at higher gas velocities. The relationship between inlet gas velocity and diameter can be represented by the following equation (Eq 10) (Towler & Sinnott, 2022).

$$D = \sqrt{\frac{4 \cdot V}{\pi \cdot \rho \cdot v}} \quad (10)$$

where  $D$  is the column diameter (m),  $V$  is the maximum vapor rate (kg/s),  $\rho$  is the density (kg/m<sup>3</sup>), and  $v$  is the maximum allowable vapor velocity, based on the gross (total) column cross-sectional area (m/s).

### 3.2.4 Effect of Stripper Murphree Efficiency on LCoC and Energy Penalty

Murphree efficiency shows a very low sensitivity to both performance indicators. The total change in LCoC is only \$0.08/ton over the efficiency range of 0.4–0.8, as shown in Figure 3 with the following linear regression equation (Eq 11).

$$\text{LCoC} = -0.2131 \times \text{Eff Murphree} - 63.191 \quad (R^2 = 0.9955) \quad (11)$$

where Eff Murphree is the murphree efficiency in stripper (dimensionless fraction). The effect of Murphree efficiency on cost depends on the cost and size of the required column. The column cost itself has an exponent with respect to height (0.3) which is much lower than the exponent with respect to diameter (1.7) (Turton et al., 2012; Smith, 2016). Since the stripper diameter is determined by vapor flooding conditions (not by Murphree efficiency), variations in efficiency only affect the packing height. Consequently, although the required packing height increases significantly, the cost impact is very limited due to the low exponent on the column height component.

Meanwhile, the change in the energy penalty is only 0.10 percentage points, as shown in Figure 4 with the following linear regression equation (Eq 12).

$$\text{EP} = -0.0012 \times \text{Eff Murphree} + 0.3045 \quad (R^2 = 0.6652) \quad (12)$$

Higher Murphree efficiency reflects actual vapor-liquid equilibrium approaching ideal conditions in each packing segment of the stripper. Under fixed reboiler temperature (120°C) and stripper pressure (2 bar) conditions, a higher Murphree efficiency means CO<sub>2</sub> is more completely desorbed per unit of packing height, thus marginally reducing the steam regeneration requirement. However, this very small decrease (0.10 percentage points for an efficiency increase from 0.4 to 0.8) indicates that the stripper in the MDEA-PZ system operates close to thermodynamic equilibrium conditions even at lower Murphree efficiencies. Rochelle (2009) explains that the stripper performance in amine systems with a piperazine promoter is more controlled by the thermodynamic limitations of solvent loading in the reboiler, rather than by the mass transfer efficiency at each stage; therefore, variations in Murphree efficiency become a secondary parameter with respect to the energy penalty.

### 3.3. Economic Analysis and Cost Structure

The economic evaluation of the CCS-EOR project was conducted using the Discounted Cash Flow method with an 8.5% discount rate and a 25-year project lifetime. CAPEX estimation employed the Enhanced Detailed Factor Method, integrated with equipment sizing results from the Aspen HYSYS simulation, consistent with the methodology applied by Pershen (2025) and Rubin et al. (2015).

#### 3.3.1 CAPEX Structure

The total project CAPEX reached \$1,315.4 million, dominated by the CO<sub>2</sub> capture, purification, and compression unit at \$1,128.9 million (85.8% of the total CAPEX). This dominance of capture unit costs is consistent with the characteristics of post-combustion capture-based CCS projects in the literature, where the capture plant accounts for 80–90% of the total system CAPEX (Rubin et al., 2015; NETL, 2015). The cost of the 50 km pipeline reached \$44.4 million (3.37%), while the cost of the injection and storage facilities amounted to \$22.6 million (1.7%).

Within the capture unit, the compression train constitutes the single largest equipment category, costing \$68.81 million (6.1% of the capture CAPEX). This is due to the substantial pressure ratio (145/2 = 72.5) from the initial pressure (2 bar) to the dense phase condition (145 bar), which requires three compression stages with a total power requirement of 72.09 MW. NETL (2015) reports that CO<sub>2</sub> compression costs are among the largest components of CCS system CAPEX, with specific compression energy ranging from 0.4–0.5 GJ/ton CO<sub>2</sub> for compression to pressures >100 bar, consistent with the value of 0.47 GJ/ton obtained in this study.

#### 3.3.2 OPEX Structure

The details of the annual OPEX are presented in Figure 6. Total annual OPEX reaches \$241.9 million, with the largest components being capture OPEX (\$161.5 million/year, 66.8%) and storage OPEX (\$78.7 million/year, 32.5%). Transport OPEX is very low (\$1.77 million/year, 0.7%) because CO<sub>2</sub> in the dense phase does not require booster compression over a distance of 50 km, consistent with literature reporting specific onshore pipeline CO<sub>2</sub> transportation costs of \$0.31–0.35/ton CO<sub>2</sub> for a 50 km distance (IEA, 2020; Li et al., 2009).

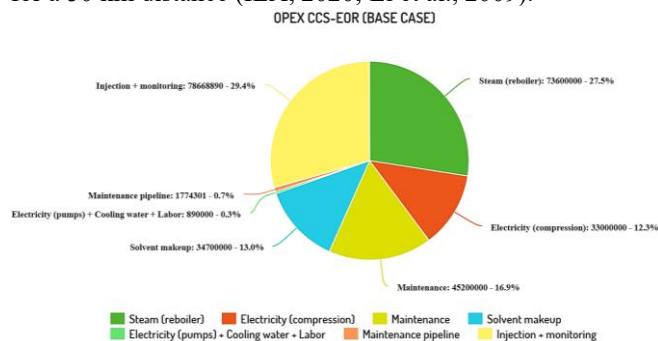


Figure 6. Percentage of OPEX (Base Case)

Within the capture OPEX components, reboiler steam cost dominates at \$73.6 million/year (45.6% of capture OPEX), consistent with the fundamental characteristic of amine-based chemical absorption processes where solvent regeneration is the most energy-intensive stage, with typical regeneration heat requirements of 3–4 GJ/ton CO<sub>2</sub> (Rochelle, 2009; Abu-Zahra et al., 2007). The PZ (piperazine) solvent makeup cost reaches a significant

\$21.5 million/year due to the piperazine price of \$8/kg, highlighting the importance of solvent degradation control in long-term operations.

### 3.3.3 Revenue Analysis and Economic Feasibility

The project's total annual revenue reaches \$735.6 million, consisting of EOR revenue of \$679.0 million (92.3%) and carbon incentive revenue of \$56.6 million (7.7%). The dominance of EOR revenue indicates that the project's economic feasibility is highly dependent on reservoir performance and oil prices. A variation of  $\pm$ \$10/bbl in oil price alters the annual revenue by  $\pm$ \$113 million/year ( $\pm$ 15%). The integration of CCS with EOR proves to be transformative, where the project's NPV with EOR reaches \$2,070 million, compared to \$1,714 million without the carbon incentive (a 17.2% decrease), and  $-$ \$2,559 million for a pure storage scenario without EOR and without carbon credits. This finding is consistent with studies by Wei et al. (2023) and the Global CCS Institute (2022) which state that CCS–EOR integration enhances economic feasibility transformatively.

The LCoC value of  $-$ \$64.53/ton CO<sub>2</sub> indicates that the project not only covers all costs but also generates a net profit of \$64.53 per ton of CO<sub>2</sub> captured. The Total Annualized Cost (TAC) of \$370.4 million/year shows that the proportion of OPEX (\$241.9 million, 64.7%) is greater than the annualized CAPEX (\$128.5 million, 35.3%), which is a common characteristic of energy-intensive processes (Rubin et al., 2015). For benchmarking purposes, the conventional LCoC defined as TAC divided by annual CO<sub>2</sub> captured, without deducting revenue for the Balanced Optimal scenario is \$65.65/ton CO<sub>2</sub>. This value is lower than the \$72.6/ton CO<sub>2</sub> reported by Adisasmito et al. (2023) for a comparable 1,000 MW Indonesian CFPP using Shell-Cansolv solvent, and the \$72/ton CO<sub>2</sub> reported by Poblete (2024), and falls within the established range of \$60–

\$100/ton CO<sub>2</sub> for post-combustion amine-based CCS (Rubin et al., 2015; IPCC, 2005).

The lower conventional LCoC in the present study is primarily attributable to the MDEA–PZ solvent blend, which achieves a specific reboiler duty of 3.08 GJ/ton CO<sub>2</sub> approximately 20–25% lower than MEA-based systems (3.7–4.2 GJ/ton CO<sub>2</sub>; Rochelle, 2009) reducing the steam cost that constitutes the dominant component of capture OPEX. When EOR revenue is incorporated, the LCoC becomes negative at  $-$ \$64.53/ton CO<sub>2</sub>, indicating that the project generates a net profit per ton of CO<sub>2</sub> captured. Poblete (2024) similarly reports a negative LCoC of  $-$ \$9.4/ton CO<sub>2</sub> when EOR revenue is included, confirming that CCS–EOR integration can convert a cost center into a profitable operation. The larger magnitude of the negative LCoC in the present study relative to Poblete (2024) is explained by the substantially higher EOR revenue stream: this study assumes an incremental oil recovery of 2 bbl/ton CO<sub>2</sub> at \$60/bbl, yielding an oil revenue of \$679 million/year (92.3% of total revenue), which far exceeds the total annualized cost of \$370.4 million/year. The difference in revenue magnitude between the two studies is attributable to differences in assumed EOR ratio, oil price, and CO<sub>2</sub> injection scale.

### 3.4. Selection and Comparison of Optimal Scenarios

The selection of optimal scenarios was conducted using a combination of four approaches: Pareto optimality analysis for the balanced scenario, single-objective optimization for the low-cost scenario, lexicographic optimization for the high-efficiency scenario, and constraint-based selection for the conservative industry scenario. The four scenarios are designed to represent a spectrum of different techno-economic objectives (Marler & Arora, 2004; Petrovic et al., 2019). The operating parameters and techno-economic performance of the four scenarios are presented in Table 6.

**Table 6.** Summary of Optimal Scenarios (Operating Parameters and Performance Indicators)

Scenario	Gas Velocity (m/s)	Eff. Murphree	$\Delta$ Tmin (°C)	CO <sub>2</sub> Removal (%)	LCoC (\$/ton)	Energy Penalty (%)	NPV (Million USD)
<i>Low Cost</i>	2.5	0.8	18	95	-66.01	30.22	2,218.949
<i>High Efficiency</i>	2.5	0.6	10	95	-65.63	28.75	2,196.737
<i>Balanced Optimum</i>	2.5	0.8	10	95	-65.65	28.75	2,197.438
<i>Constraint Based</i>	2.5	0.8	10	90	-64.53	28.91	2,070.178

The Low-Cost Scenario has the most negative LCoC ( $-$ \$66.01/ton), indicating the highest profitability per ton of CO<sub>2</sub>. However, this profitability is achieved using a larger  $\Delta$ Tmin of 18°C, resulting in lower internal heat recovery and the highest energy penalty (30.22%). Both the High-Efficiency and Balanced Optimal Scenarios achieve the same lowest energy penalty (28.75%) with an absolute energy consumption of 287.5 MW using a  $\Delta$ Tmin of 10°C. The difference between them lies in the Murphree efficiency, with a very small NPV difference of only \$0.7 million (0.03%).

The Balanced Optimal Scenario is recommended as the primary configuration because it offers the best balance between profitability and energy efficiency, with an LCoC

of  $-$ \$65.65/ton (a gap of only 0.54% from the Low-Cost scenario), an energy penalty of 28.75% (the lowest, tied with the High-Efficiency scenario), an NPV of \$2,197 million, and it utilizes a Murphree efficiency of 0.8, representing the performance of modern structured packings such as Mellapak 250Y or Flexipac 2Y, which are technologically achievable (Pershen, 2025). The improvement from the Constraint-Based scenario (90% removal) to the Balanced Optimal scenario (95% removal) results in an incremental NPV of \$127.2 million with an incremental CAPEX of \$34.7 million, equivalent to a payback period of only 1.5 years. This confirms that targeting maximum CO<sub>2</sub> capture (95%) is a reasonably

sound economic strategy for CCS-EOR applications with strong revenue streams (Petrovic et al., 2019).

All scenarios exhibit high NPVs within a narrow range (\$2,070–\$2,219 million), with a coefficient of variation of only 3.4%. This economic robustness stems from the dominance of EOR revenue (\$679 million/year), which far exceeds the total TAC (\$370–\$379 million/year), thereby creating a large profitability margin that is resilient to variations in operating parameters.

### 3.5. Evaluation of the Effect of Pipeline Distance

The CO<sub>2</sub> transportation distance from the capture facility to the EOR injection site is a critical parameter affecting the project's economic feasibility. The analysis was conducted for four representative distances (50, 100, 150, and 200 km) across the four optimal scenarios. Pipeline costs were calculated using a cost correlation approach based on diameter, distance, and material, with pipeline specifications of 450 mm (18 inch, Schedule 140) diameter, made of X45/X80 carbon steel grade for CO<sub>2</sub> in the dense phase condition (145 bar, 29°C).

**Table 7.** NPV of the Four Scenarios at Various Pipeline Distances

Scenario	NPV at each distance (million USD)			
	50 km	100 km	150 km	200 km
<i>Low Cost</i>	2,218.9	2,166.7	2,144.3	2,061.9
<i>High Efficiency</i>	2,196.7	2,144.5	2,092.1	2,039.7
<i>Balanced</i>	2,197.4	2,145.2	2,092.8	2,040.4
<i>Optimum</i>				
<i>Constraint Based</i>	2,070.2	2,018.1	1966	1,913.9

The effect of pipeline distance on the NPV of the four scenarios is presented in Table 7. All scenarios show an identical decrease in NPV of \$157 million (7.1%) for an increase in distance from 50 km to 200 km. This identical decrease indicates that transportation costs do not interact significantly with the capture system's operating parameters, so the relative ranking among scenarios does not change with increasing distance.

The NPV remains consistently positive and large (> \$1.9 billion) across all scenarios and distances analyzed. No critical distance was found where economic feasibility decreases drastically within the 50–200 km range. This is due to the dominance of capture and storage costs (>90% of total CAPEX and OPEX) compared to transportation costs, as well as the substantial EOR revenue which far exceeds total project costs. With the LCoC remaining negative in the range of –\$58 to –\$66/ton depending on the scenario and distance, the project is deemed economically robust against variations in storage location.

The specific CO<sub>2</sub> transportation cost for the 50 km base case, amounting to \$0.31–\$0.35/ton CO<sub>2</sub>, is consistent with the literature for onshore CO<sub>2</sub> pipelines (IEA, 2020; Li et al., 2009) and is significantly lower than the capture cost (\$29/ton CO<sub>2</sub>). Aspelund et al. (2006), in their

comprehensive study on CO<sub>2</sub> transport infrastructure, also concluded that onshore pipeline transportation costs are incremental and do not dominate the total CCS project costs compared to capture costs. This finding provides substantial flexibility in selecting a storage site without compromising the fundamental economic feasibility of the project, as long as the transportation distance remains within the analyzed range.

## 4. Conclusions

This study demonstrates that the integration of post-combustion CCS with CO<sub>2</sub>-EOR for a 1,000 MW ultra-supercritical coal-fired power plant in Indonesia is both technically feasible and economically profitable, providing quantitative end-to-end evidence that remains limited in the literature for the context of developing countries. Through Python–Aspen HYSYS automation evaluating 162 parameter combinations without convergence failure, the four Pareto-optimal scenarios identified consistently yield negative LCoC values (–\$65.63 to –\$66.01/ton CO<sub>2</sub>) and NPVs of \$2.07–\$2.22 billion, confirming that EOR revenue can convert a CCS system from a cost center into a source of profitability. The Balanced Optimal scenario, featuring 95% CO<sub>2</sub> recovery, a  $\Delta T_{min}$  of 10°C, a Murphree efficiency of 0.8, an inlet gas velocity of 2.5 m/s, and a solvent blend of 35 wt% MDEA + 15 wt% PZ, is recommended for implementation as it offers the lowest energy penalty (28.75%), an LCoC of –\$65.65/ton CO<sub>2</sub>, and an NPV of \$2.20 billion, with all operating parameters being commercially proven. A key scientific finding, contrary to general expectations, is that increasing CO<sub>2</sub> recovery from 90% to 95% actually lowers specific energy consumption due to the interaction between the fixed reboiler temperature constraint and the thermodynamic loading profile of the MDEA-PZ solvent, challenging the assumption that higher capture targets always result in a greater energy penalty. Robustness analysis also shows that the NPV remains viable up to a pipeline distance of 200 km, extending the geographical applicability of this study's results.

Future research should prioritize experimental validation of the non-monotonic energy consumption phenomenon through pilot-scale testing with MDEA-PZ solvent on actual coal power plant flue gas in Indonesia, as well as extending the analysis to CO<sub>2</sub> removal rates above 95% to establish diminishing returns points in planning near-zero emission pathways. The modeling framework developed in this study has the potential to be adapted for other high-emission sectors such as the cement and steel industries, and for alternative CO<sub>2</sub> utilization pathways like methanol synthesis, thereby enabling more comprehensive cross-sectoral economic comparisons in support of the national industrial decarbonization strategy aligned with Indonesia's 2060 net-zero target.

## Acknowledgements

This research is funded by Institut Teknologi Sepuluh Nopember (ITS) and managed under the Strategic Research Grant (SRG) Type D Scheme (Contract No. 1687/PKS/ITS/2026).

### Statement

This manuscript was edited for language clarity using AI-assisted tools (DeepSeek) under the direct supervision of the authors. No part of the scientific analysis, data processing, modelling, or interpretation was generated by AI. All scientific content, results, and conclusions were fully produced and verified by the authors.

### CRedit authorship contribution statement

**Raden Ricko Satriyo:** Writing – review & editing, Validation, Methodology, Software.

**Renanto:** Supervision, Conceptualization, Writing – review & editing.

**Rendra Panca Anugraha:** Funding acquisition, Supervision, Methodology

**Roudlotus Salwa Aulia:** Writing – original draft, Visualization, Software.

**Galuh Ferlianes Lestari:** Software, Resources, Formal analysis.

### Declaration of competing interest

The authors declare that they have no known competing financial interests or personal relationships that could have appeared to influence the work reported in this paper.

### Data availability

The data that support the findings of this study are available upon request.

### References

- Abu-Zahra, M., Schneiders, L., Niederer, J., Feron, P., & Versteeg, G. (2007). CO<sub>2</sub> capture from power plants Part I. A parametric study of the technical performance based on monoethanolamine. *CO<sub>2</sub> Capture from Power Plants Part I. A Parametric Study of the Technical Performance Based on Monoethanolamine*, 1. [https://doi.org/10.1016/S1750-5836\(06\)00007-7](https://doi.org/10.1016/S1750-5836(06)00007-7)
- Adisasmito, S., Raksajati, A., Ali, A., Susilo, H., Susetyo, M. A., & Reza, A. M. (2023). Modelling of carbon capture process for coal-fired power plants in Indonesia. *Chemical Engineering Transactions*, 106, 961–966. <https://doi.org/10.3303/CET23106161>
- Aspelund, A., Mølnvik, M. J., & De Koeijer, G. (2006). Ship Transport of CO<sub>2</sub>. *Chemical Engineering Research and Design*, 84(9), 847–855. <https://doi.org/10.1205/cherd.5147>
- Bishnoi, S., & Rochelle, G. T. (2000). Absorption of carbon dioxide into aqueous piperazine: Reaction kinetics, mass transfer, and solubility. *Chemical Engineering Science*, 55(22), 5531–5543. [https://doi.org/10.1016/S0009-2509\(00\)00182-2](https://doi.org/10.1016/S0009-2509(00)00182-2)
- Boot-Handford, M. E., Abanades, J. C., Anthony, E. J., Blunt, M. J., Brandani, S., Mac Dowell, N., Fernández, J. R., Ferrari, M. C., Gross, R., Hallett, J. P., Haszeldine, R. S., Heptonstall, P., Lyngfelt, A., Makuch, Z., Mangano, E., Porter, R. T. J., Pourkashanian, M., Rochelle, G. T., Shah, N., ... Fennell, P. S. (2014). Carbon capture and storage update. *Energy & Environmental Science*, 7(1), 130–189. <https://doi.org/10.1039/C3EE42350F>
- Bui, M., Adjiman, C. S., Bardow, A., Anthony, E. J., Boston, A., Brown, S., Fennell, P. S., Fuss, S., Galindo, A., Hackett, L. A., Hallett, J. P., Herzog, H. J., Jackson, G., Kemper, J., Krevor, S., Maitland, G. C., Matuszewski, M., Metcalfe, I. S., Petit, C., ... Mac Dowell, N. (2018). Carbon capture and storage (CCS): The way forward. *Energy & Environmental Science*, 11(5), 1062–1176. <https://doi.org/10.1039/C7EE02342A>
- Febriani, A. V., Hanum, F. F., Kuncara, J., & Setyawan, M. (2024). Optimalisasi mutu batubara Indonesia. *\*Eksergi\**, 21(2), 70–76. <https://doi.org/10.31315/e.v21i2.11761>
- Global CCS Institute. (2022). *Global status of CCS 2022*. Global CCS Institute.
- Government of Indonesia. (2022). *Enhanced nationally determined contribution: Republic of Indonesia*.
- Handogo, R., Mualim, A., Sutikno, J. P., & Altway, A. (2022). Evaluation of CO<sub>2</sub> transport design via pipeline in the CCS system with various distance combinations. *ECS Transactions*, 107, 8593–8608. <https://doi.org/10.1149/10701.8593ecst>
- International Energy Agency (IEA). (2020). *CCUS in clean energy transitions*. IEA. <https://www.iea.org/reports/ccus-in-clean-energy-transitions>
- International Energy Agency. (2021). *Net zero by 2050: A roadmap for the global energy sector* (4th rev. ed.).
- International Energy Forum (IEF). (2021). *Carbon capture, utilization and storage: Policy, markets, and investment pathways*. IEF. <https://www.ief.org>
- Institute for Essential Services Reform (IESR). (2024, June 14). *Coal Domination in Indonesia, What are the Opportunities for Sustainable Energy?*. <https://iesr.or.id/en/coal-domination-in-indonesia-what-are-the-opportunities-for-sustainable-energy/>
- Intergovernmental Panel on Climate Change (IPCC). (2005). *IPCC special report on carbon dioxide capture and storage*. Cambridge University Press.
- Irfan, & Tobing, S. (2021). *Analysis energy penalty implementation technology CO<sub>2</sub> capture post combustion in existing coal fired power plant class 660 MW*. SSRN. <https://ssrn.com/abstract=4874726>
- Jarrell, P. M., Fox, C. E., Stein, M. H., & Webb, S. L. (2002). *Practical aspects of CO<sub>2</sub> flooding* (Monograph Vol. 22). Society of Petroleum Engineers.

- Kementerian Energi dan Sumber Daya Mineral (ESDM). (2025). *Penetapan harga minyak mentah Indonesia*. Kementerian ESDM Republik Indonesia.
- Li, H., Yan, J., Yan, J., & Anheden, M. (2009). Impurity impacts on the purification process in oxy-fuel combustion based CO<sub>2</sub> capture and storage system. *Applied Energy*, 86(2), 202–213. <https://doi.org/10.1016/j.apenergy.2008.05.006>
- Lucquiaud, M., & Gibbins, J. (2011). On the integration of CO<sub>2</sub> capture with coal-fired power plants: A methodology to assess and optimise solvent-based post-combustion capture systems. *International Journal of Greenhouse Gas Control*, 5(3), 427–438. <https://doi.org/10.1016/j.cherd.2011.03.003>
- Mahidin, Maulana, F., Mukramah, Adisalamun, Hisbullah, Hadi, A., MH, N., & Abnisa, F. (2025). Achieving Net Zero Emissions Target: Development of Carbon Dioxide Handling Technologies, Its Challenges and Barriers. *Eksergi*, 22(2), 150–157. <https://doi.org/10.31315/eksergi.v22i2.14655>
- Marler, R. T., & Arora, J. S. (2004). Survey of multi-objective optimization methods for engineering. *Structural and Multidisciplinary Optimization*, 26(6), 369–395. <https://doi.org/10.1007/s00158-003-0368-6>
- National Energy Technology Laboratory (NETL). (2015). *Cost and performance baseline for fossil energy plants, volume 1: Bituminous coal and natural gas to electricity* (DOE/NETL-2015/1723). U.S. Department of Energy.
- Nyamiati, R. D., Nurkhamidah, S., Nanda, D. E., Timotius, D., Mahreni, M., Handayani, D. P., & Krisnabudhi, A. (2023). Current research on the development of carbon separation and capture with polymeric membrane: A state of the art review. *Eksergi*, 20(2), 58–63. <https://doi.org/10.31315/e.v20i2.9096>
- Pamungkas, R. Y., Nurkhamidah, S., Taufany, F., Altway, A., Susianto, & Rahmawati, Y. (2025). Effect of DEA solvent flow rate on CO<sub>2</sub> absorption-desorption. *Eksergi\**, 22(3), 167–174. <https://doi.org/10.31315/eksergi.v22i3.14951>
- Park, K., & Øi, L. E. (2017). Optimization of gas velocity and pressure drop in CO<sub>2</sub> absorption column. In *Proceedings of the 58th Conference on Simulation and Modelling (SIMS 58)* (pp. 292–297). Linköping University Electronic Press. <https://doi.org/10.3384/ecp17138292>
- Peletiri, S. P., Rahmanian, N., & Mujtaba, I. M. (2017). Effects of impurities on CO<sub>2</sub> pipeline performance. *Chemical Engineering Transactions*, 57, 355–360. <https://doi.org/10.3303/CET1757060>
- Peletiri, S. P., Rahmanian, N., & Mujtaba, I. M. (2018). CO<sub>2</sub> Pipeline Design: A Review. *Energies*, 11(9), 2184. <https://doi.org/10.3390/en11092184>
- Pershen, S. (2025). Process simulation combined with other calculation tools for automated cost optimization of CO<sub>2</sub> capture [Master's thesis]. University of South-Eastern Norway.
- Petrovic, D., Anicic, B., & Gvozdenac, D. (2019). Optimization of Post Combustion CO<sub>2</sub> Capture from a Combined-Cycle Gas Turbine Power Plant via Taguchi Design of Experiment. *Processes*, 7(6), 364. <https://doi.org/10.3390/pr7060364>
- Poblete, J., de Medeiros, J. L., & Araújo, O. Q. F. (2024). *Thermodynamically efficient, low-emission gas-to-wire for carbon dioxide-rich natural gas: Exhaust gas recycle and Rankine cycle intensifications*. *Processes*, 12(4), 639. <https://doi.org/10.3390/pr12040639>
- PT PLN (Persero). (2025). *Tarif tenaga listrik PT PLN (Persero) tahun 2025*. PT PLN (Persero).
- Rochelle, G. T. (2009). Amine scrubbing for CO<sub>2</sub> capture. *Science*, 325(5948), 1652–1654. <https://doi.org/10.1126/science.1176731>
- Rochelle, G. T., Chen, E., Freeman, S., Van Wagener, D., Xu, Q., & Voice, A. (2011). Aqueous piperazine as the new standard for CO<sub>2</sub> capture technology. *Chemical Engineering Journal*, 171(3), 725–733. <https://doi.org/10.1016/j.cej.2011.02.011>
- Rubin, E. S., Davison, J. E., & Herzog, H. J. (2015). The cost of CO<sub>2</sub> capture and storage. *International Journal of Greenhouse Gas Control*, 40, 378–400. <https://doi.org/10.1016/j.ijggc.2015.05.018>
- Shirdel, S., Øi, L. E., Aromada, S. A., & Eldrup, N. H. (2022). Sensitivity analysis and cost estimation of a CO<sub>2</sub> capture plant in Aspen HYSYS. *ChemEngineering*, 6(2), 28. <https://doi.org/10.3390/chemengineering6020028>
- Smith, R. (2016). *Chemical process design and integration* (2nd ed.) (pp. 493–495). Wiley.
- Sultan, H., Bhatti, U.H., Muhammad, H.A., Nam, S.C., Baek, I.H., 2021. Modification of postcombustion CO<sub>2</sub> capture process: a techno-economic analysis. *Greenh. Gases Sci. Technol.* 11, 165–182. <https://doi.org/10.1002/ghg.2042>
- Sussatrio, H., Hadiyanto, H., & Widayat, W. (2024). Optimasi Komposisi MDEA dan MEA Sebagai Absorbent untuk Proses Penghilangan CO<sub>2</sub> dalam Produksi Gas di Lapangan A. *Eksergi*, 21(1), 29. <https://doi.org/10.31315/e.v21i1.10855>
- Towler, G., & Sinnott, R. (2022). *Chemical engineering design: Principles, practice and economics of plant and process design* (3rd ed.) (pp. 667). Butterworth-Heinemann Inc.
- Turton, R., Bailie, R. C., Whiting, W. B., & Shaeiwitz, J. A. (2012). *Analysis, synthesis, and design of chemical processes* (4th ed.) (pp. 207). Prentice Hall.
- Wei, B., Wang, B., Li, X., Aishan, M., & Ju, Y. (2023). CO<sub>2</sub> storage in depleted oil and gas reservoirs: A review. *Advances in Geo-Energy Research*, 9(2), 76–93. <https://doi.org/10.46690/ager.2023.08.02>
- Yasmin, K. A. (2021). *Reservoir simulation and economic model evaluation for CO<sub>2</sub> sequestration in depleted*

**Citation:** Satriyo, R. R., Renanto, Aulia, R. S., & Lestari, G. F. Techno-Economic Sensitivity Analysis of Integrated CCS–EOR for a 1,000 MW Ultra-Supercritical Coal-Fired Power Plant in Indonesia. *Eksergi*, 23(2), 58–61

*gas reservoir of field X* (Bachelor's thesis, Institut Teknologi Bandung).